

Design of a Nitrous Oxide/Isopropyl Alcohol Regeneratively Cooled Liquid Rocket Engine for Additively Manufacturing

Kat Chen, Daniel Kolano, Mitchell Miya, Denis Profka



The authors are with the Department of Mechanical Engineering, Columbia University, New York, NY: ksc2155@columbia.edu, mkm2201@columbia.edu, dkw2117@columbia.edu, dp2904@columbia.edu. This material is based upon work developed in the MECE E3420 / E3430 Engineering Design Courses

Abstract—By leveraging the advantages of 3D Direct Metal Laser Sintering (DMLS), the authors designed a 600 lbf-thrust nitrous oxide/isopropyl alcohol regeneratively cooled rocket engine of a scale suitable for service in the small satellites market. Once fired, this engine will be the first such engine to have been manufactured and tested. The design leveraged analytical and numerical modelling in concert with the enlarged design space afforded by the additive manufacturing process to create an engine with low mass and high efficiency through optimized flow paths and cooling channel sizings, reduced interface count, and small injector orifices for improved atomization and combustion efficiency. The design was successfully manufactured and cold flow tested with water, and will continue to move towards static fire testing in the coming year.

I. INTRODUCTION

Historically, creating a rocket engine was a labor-intensive process that took an enormous amount of time and effort to complete because of the low machinability of the material used and the intricate geometry needed in the design. However, times have certainly changed since then and so has the rocket engine market.

The small satellite market is projected to grow from 2.8 to 7.1 billion USD from 2020 to 2025 in the world market. [1]. This will require small rocket engines that are designed for this task and have the necessary capabilities. Engines will need to have several firing cycles and they will need to be efficient. To meet the increased demand, the engines need to have a rapid design and manufacturing cycle, while meeting design standards that may vary from engine to engine. These requirements cannot be met without the use of 3d metal printing.

3D metal printing is advantageous because it dramatically reduces production time compared to traditional manufacturing methods. [2]. It allows for much greater design freedom, allowing the creator to make a rocket that has much less weight and higher combustion efficiency, leading to a more efficient rocket. Because of the typical size and intricate internal geometry of small rocket engines, additive manufacturing is the perfect method of making them.

The team set out to create a novel design for a rocket engine that could be used for the small satellite market. The rocket engine's base design constraints were set by the requirement that it satisfy the thrust profile needed for Columbia Rocketry's entry into the Spaceport America Cup Student Launch Competition. Additionally, the team was also fortunate enough to secure a sponsorship with 3D systems allowing us to leverage their DMLS 3D metal printer in order to create a prototype of our design.

The two primary components of a small rocket engine are the injector and combustion chamber, which can be seen on a rendering of our prototype in Figure 1, and the completed printed parts in Figure 2. The injector regulates and directs the flow of fuel and oxidizer into the combustion chamber, rendering it essential for maintaining stable and efficient combustion. Meanwhile the combustion chamber is where the combustion process actually occurs. In our case the chamber is also combined with the nozzle, in which adiabatic expansion of the combustion products accelerates them to

supersonic speeds to provide thrust. Finally, our engine implements a method known as regenerative cooling, in which one of the propellants (in our case the fuel) flows through the walls of the combustion chamber and nozzle before being sent into the injector in order to exchange heat through the combustion chamber wall, thus allowing the chamber to operate in a steady-state despite the combustion temperatures of several thousand degrees Kelvin far exceeding material limits.

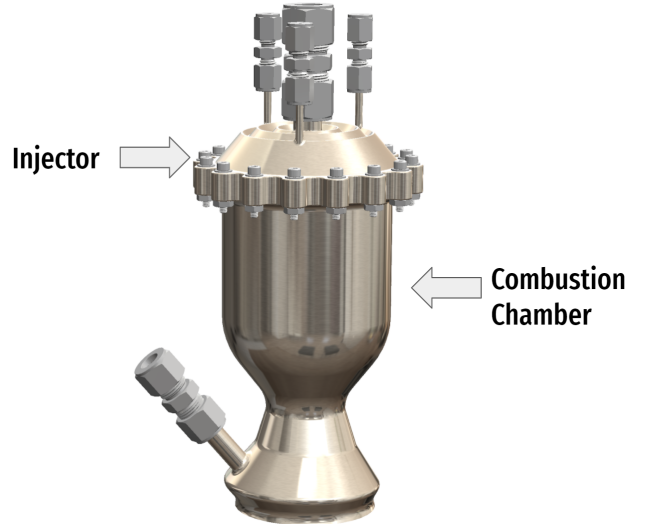


Fig. 1. The two primary components of a rocket engine, the injector and combustion chamber



Fig. 2. The completed additively manufactured injector (left) and combustion chamber (right) of our rocket engine

The complete fluid flow path through both the chamber and injector can be seen in Figure 3. From this figure, one can see that without additive manufacturing, just designing something manufacturable would be the primary concern due to the need for a host of precise internal geometries and orifices. However additive manufacturing opened up a host of possibilities for novel design and optimization previously

impossible with traditional techniques.

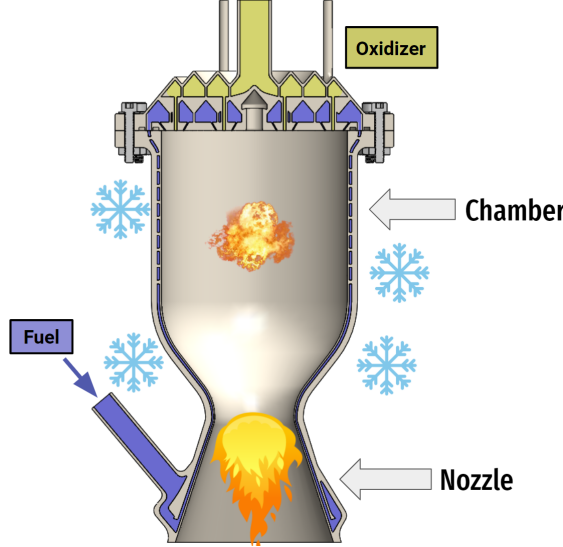


Fig. 3. A cross-section of our rocket engine, showing the fuel flow paths in purple and oxidizer flow paths in yellow, as well as the location of combustion inside the chamber, and the flow path out the nozzle

II. METHODS

A. General Engine Design

To begin the design of the engine, we chose several design parameters based on the project goals and the resources available to us. These parameters are given in Table I. First and foremost, rocket engines require a fuel and oxidizer as propellants. Nitrous oxide was chosen as an oxidizer primarily due to the team's and school's previous experience with the fluid, which removed technical and bureaucratic barriers such as obtaining suitable containers and valves as well as university permissions for its use that would have been present with the other common oxidizer, liquid oxygen. Additionally, as nitrous oxide is self-pressurizing due to its high vapor pressure, no additional pressurant tank would be needed for the oxidizer, greatly reducing fluid system complexity. Isopropyl alcohol was chosen as a fuel for its availability, stability, and generally good performance in combination with nitrous oxide.

TABLE I

THE UNCONSTRAINED DESIGN PARAMETERS WE CHOSE TO USE FOR OUR ENGINE

Parameter	Value
Fuel	Isopropyl Alcohol
Oxidizer	Nitrous Oxide
Thrust	600 lbf
Chamber Pressure	400 psi

The engine thrust was chosen to match the thrust needed for Columbia Rocketry's entry into the IREC Student Launch Competition, as the engine is hoped to eventually be used in this rocket. Meanwhile, the chamber pressure was chosen so as to be as high as possible without exceeding the level needed to maintain choked flow of oxidizer through the injector, generally about 80% of the pressure upstream of the injector [3], which would be dictated by the vapor pressure of the oxidizer at a given temperature, which can be seen in figure 4. To ensure choked flow throughout the burn, even

as the nitrous oxide temperature and thus vapor pressure is reduced through vaporization over the course of the burn, we selected a chamber pressure of 400 psi, which gives margin to maintain choked flow down to a temperature of 5 degrees Celsius, which is 5 degrees below the lowest recorded temperature we have seen during test firings of Columbia's hybrid rockets.

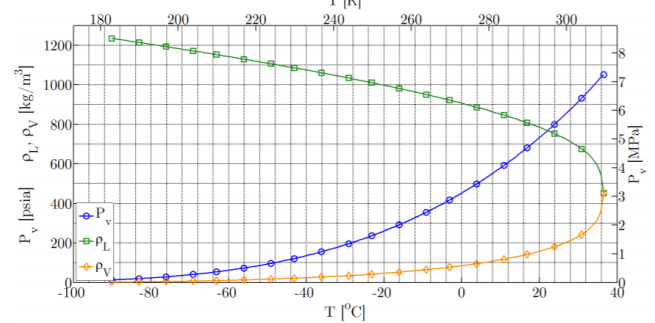


Fig. 4. The variation of vapor pressure P_V , vapor density ρ_V , and liquid density ρ_L of nitrous oxide with temperature as given in [3].

Once these parameters were selected, the remainder of the engine design specifications could be calculated by roughly following the procedures outlined in rocket engine design texts such as Huzel and Huang's in "Design of Liquid Propellant Rocket Engines" [4]. NASA's Chemical Equilibrium with Applications (CEA) software was used to find combustion parameters such as adiabatic flame temperature, combustion product specific heat ratio, and ideal specific impulse (eq 1). Once these parameters were calculated, hand calculations in addition to some intuition based on previous experience could be used to calculate many important parameters.

For example, to calculate our required propellant mass flow rate, we can use the ideal specific impulse calculated from the propellant chemical properties:

$$I_{sp,ideal} = \frac{F}{\dot{m}_{propellants}g} \quad (1)$$

Where F is the engine thrust, g is the gravitational constant, and $\dot{m}_{propellants}$ is the overall propellant mass flow rate. However, this value will generally never be reached in practice, so a correction factor known as the overall efficiency $\eta_{overall}$ is added to estimate the actual delivered specific impulse $I_{sp,adjusted} = \eta_{overall} I_{sp,ideal}$. This overall efficiency is calculated as the product of an estimated combustion efficiency η_{c*} and nozzle efficiency η_{nozzle} . The combustion efficiency was estimated based on previous experience with engines of this type as well as a literature search, and a conservative value of 0.90 was chosen to avoid underperformance which would preclude use of the engine in an active rocket. The nozzle efficiency was taken as 0.97 based on the nozzle loss table for conical nozzles given in [?]. Combined, this allowed us to calculate our required propellant flow rate using equation 2.

$$\dot{m}_{propellants} = \frac{F}{\eta_{c*} \eta_{nozzle} I_{sp,ideal} g} \quad (2)$$

The remaining design parameters were calculated in a similar manner and the most prominent are given in Table II

TABLE II

THE CALCULATED DESIGN PARAMETERS OF OUR ENGINE

Parameter	Value
Nozzle Throat Diameter	1.17 in
Nozzle Exit Diameter	2.34 in
Overall Propellant Mass Flow Rate	1.411 kg/s
Fuel Mass Flow Rate	0.353 kg/s
Oxidizer Mass Flow Rate	1.058 kg/s
$I_{sp,adjusted}$	193 s
Overall Height	7.5 in
Diameter	4.0 in

B. Ensure Adequate Engine Cooling

To ensure adequate engine cooling, we carefully designed and analyzed the engine's cooling channels. As the regenerative cooling process involves a complex coupling between the fluid flow, wall temperature, and combustion properties, an iterative regenerative cooling simulation was developed in Python to model the cooling process as accurately as possible, including effects such as subcooled nucleate boiling and wall roughness which can be extremely important at high heat fluxes and in additively manufactured channels.

This model was verified as best possible using hand calculations at several chosen axial chamber locations, namely the nozzle throat (area of highest heat flux), nozzle entrance, and mid-chamber sections. Additionally, the calculated pressure drop was corroborated with CFD simulation using ANSYS Fluent, with associated mesh convergence study.

Once validated, this tool was used to iteratively determine the ideal number and shape of cooling channels at each axial location to maintain adequate cooling, minimize pressure drop, and maintain manufacturing margin.

In addition to our analytical models, based on some previous experience with regenerative cooling design, we chose to introduce a cooling channel design in which the channels spiral around the barrel section of the combustion chamber, as can be seen in the cutaway view in Figure 5. This design is meant to ensure that even given some radial asymmetry in the combustion chamber, a positive feedback loop will not be formed between an individual channel location and injector element causing a runaway temperature spike and thus a hot-spot at a single location in the chamber.

C. Ensure High-Efficiency Combustion

The design of the injector is essential to ensuring stable, efficient combustion. As mentioned before, it is responsible for passively controlling the mass flow rates of the propellant into the combustion chamber. After performing a trade study with a number of injection methods, we chose a fuel-oxidizer-fuel (OFO) triplet impinging pattern, shown in figure 6. Note that compared to the figure, our injector has the fuel and oxidizer manifolds reversed.

Because of the difficulty of modeling two phase compressible flows into the combustion chamber, we used semi-empirical equations to calculate our oxidizer mass flow rate [3]. Below is the equation used.



Fig. 5. Cutaway view of the cooling channel geometry, with fluid volumes in red

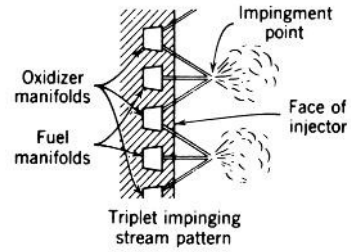


Fig. 6. Triplet impinging pattern

$$\dot{m} = NC_d A_2 \sqrt{2\rho_1[P_1 - (1-C)P_v]} \quad (3)$$

Where \dot{m} is the mass flow rate in kg/s, N is the number of orifices, C_d is an empirically determined discharge coefficient, A_2 is the area of the orifice, ρ_1 is the density of the propellant, P_1 is the pressure upstream of the orifice, C is an empirical coefficient that simulates the decrease of vapor pressure as the tank is emptied, and P_v is the vapor pressure. Note that because we were not relying on an external pressurant for our oxidizer, $P_1 = P_v$.

A number of other efficiency and stability considerations were taken into account when designing our initial versions of the injector. Our orifices were sized as small as possible to ensure proficient atomization of our propellants while still being machinable. We had a slightly outwards bias to reduce the chance for fluid stagnation areas caused by low pressure zones. We had an inwards momentum angle to reduce the amount of propellant coming into contact with our chamber walls. A specific orifice pattern was chosen to reduce the possibility for tangential combustion instability modes. Finally, we increased our fuel to oxidizer ratio of the triplet elements near the chamber walls to keep them cooler.

D. Manufacturing

For primary manufacturing of our injector and combustion chamber, we relied on our sponsor 3D Systems, who produced the parts from Inconel 718 using Direct Metal Laser Sintering (DMLS). However we did have to ensure that our part would be suitable for manufacture using the processes available. Therefore throughout the design of each part, draft analyses were performed to ensure overhang limits were obeyed and wall thicknesses and orifice diameters were sized to 3D Systems' guidelines as given in Table III. On completion of the design, a review was held with 3D Systems to ensure manufacturability of all parts, in addition to a design review with the team of rocket engine designers at Agile Space Industries which focused on approval of the overall engine design and analysis before manufacturing could begin.

TABLE III

CONSTRAINTS ON ADDITIVELY MANUFACTURED PARTS USING THE CHOSEN PROCESS AND MATERIAL (DMLS AND INCONEL 718)

Parameter	Constraint
Overhang Angle	≤ 40 degrees
Wall Thickness	≥ 0.01 inches
Orifice Diameter	≥ 0.01 inches

E. Post-Processing

Although the additive manufacturing process did make the part manufacturing process far easier, there were still several steps that needed to be taken before the injector and combustion chamber would be ready for testing. Due to their large overhang angle and requirement of low surface roughness, the o-ring grooves could not be printed in place and needed to be post-machined. Additionally, due to the high print surface roughness, each of the inlet and instrumentation tubes needed to be heavily polished before Swagelok fittings could be attached.

F. Cold Flow Testing

To ensure the manufactured part matched the design, we performed cold flow testing with water as a working fluid. The primary goal of these tests were to ensure there were no leaks in the part, the fittings we attached, or the o-ring grooves machined, check for leaks between the fuel and oxidizer flow paths, ensure proper impingement of the fuel and oxidizer elements, and check for flow asymmetry in any region.

To perform these tests, we arranged a set of fittings such that the engine could be connected to the sink in the Columbia Mechanical Engineering shop, and used this flow to perform the tests. Additionally, we designed and 3D printed a jig which would allow us to run water directly into the fuel manifold without the combustion chamber attached, which would obstruct our view of the streams produced.

III. RESULTS

This section has your main findings from your methods. You should not interpret the results here, just present them. You might choose to organize your numerical data in a table. I would recommend generate tables in Latex using <https://www.tablesgenerator.com/>

A. Regenerative Cooling Modelling

The resulting simulated wall temperature profiles and coolant temperature profiles calculated by the custom numerical code are given in figures 7 and 8.

Simulated Temperature Profiles

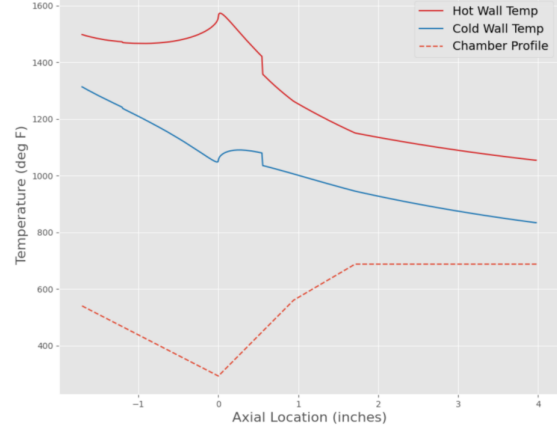


Fig. 7. Simulated profiles of the hot (on the side of the combustion chamber gasses) and cold (on the walls of the cooling channels) wall temperatures with respect to engine axial location in steady-state.

Simulated Coolant Temperature Profile

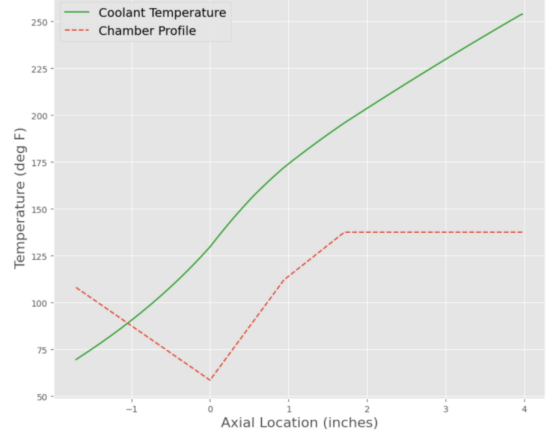


Fig. 8. Simulated profiles of the coolant temperature temperature with respect to engine axial location in steady-state.

These profiles show a maximum wall temperature of 1600 degrees Fahrenheit which occurs at the nozzle throat and a final coolant temperature of 250 degrees Fahrenheit after cooling is completed.

B. Injector Modelling

To drive our iterative design process of the injector, we performed a number of CFD simulations to both validate our hand calculations and to ensure we were not getting any unexpected flow patterns. The results of our the simulation with our final element pattern is shown below.

As seen in 9, our mass flow rate is at most 1% off nominal.

We also performed a thermal-structural analysis of the forces on our injector to ensure that combustion pressures would not compromise our o-rings. The results of the simulation are shown below, with the deformations being highly exaggerated in the image. With these results, we were able to select the correct o-ring sizes.

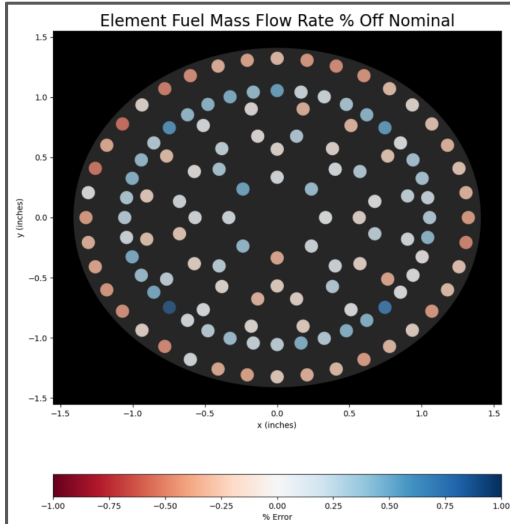


Fig. 9. Mass flow rate error across all injector elements.

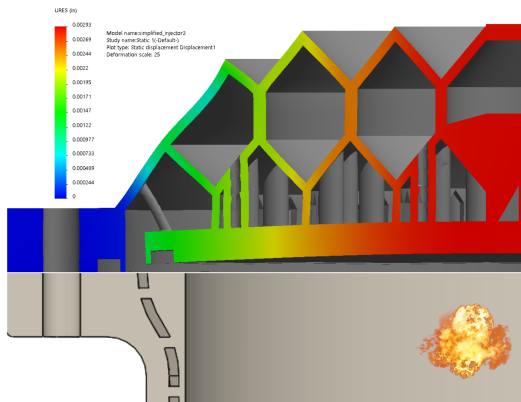


Fig. 10. Deformation analysis of injector o-ring grooves

C. Cold Flow Testing

Images of our cold flow tests are shown below.



Fig. 11. Ox cold flow

Figure 11 shows the results of our oxidizer cold flow test. No stray impinging streams from the fuel orifices are seen, suggesting that there are no leaks between our fuel and oxidizer manifolds.



Fig. 12. Ox and fuel cold flow

Figure 12 shows a test of both our fuel and oxidizer elements. Upon visual inspection, we saw that each of our triplet impinging streams were coming into contact with one another at expected impingement distances.



Fig. 13. Full assembly cold flow

Finally, figure 13 shows our full assembly attached to our cold flow set up. No leaks were observed between the injector and combustion chamber.

While these tests were performed at pressures lower than expected for our engine, they serve as a basis for future cold flow tests at expected operating pressures in the future.

D. Manufacturing

The completed printed parts, as seen in Figure 2, displayed very smooth surface finish for 3D printed material as the parts were made using a newly updated method from 3D Systems. However, there was still a great deal of surface roughness in many areas, generally concentrated in areas of high overhang angle, however with proper polishing in post-processing these rough areas were easily removed where necessary (such as on tube stubs and inside the nozzle). Additionally, all tolerances were met which ensured that all interfaces and seals aligned as expected.

IV. DISCUSSION & CONCLUSION

This is the section where you interpret your results. Discuss the consequences of your results, and the effect on your design choices. Discuss shortcomings of your analysis and how it could be improved. Where possible, compare your results to findings in literature. You should also have a closing paragraph summarizing the work.

A. Regenerative Cooling Modelling

The results of our regenerative cooling modelling gave good confidence that our engine will be able to operate in a steady-state condition for extended periods. The finding that the maximum hot wall temperature is achieved at the nozzle throat is expected as this is the region of a rocket engine where the highest heat flux is achieved due to high flow velocity and density. However the peak of slightly below 1600 F still leaves some margin in remaining strength of Inconel 718 as can be seen in the strength vs temperature curve in Figure 14. Moreover, as the simulation did not account for axial heat transfer, the peak temperature is expected to be slightly lower than that given by the simulation, further increasing the design margin.

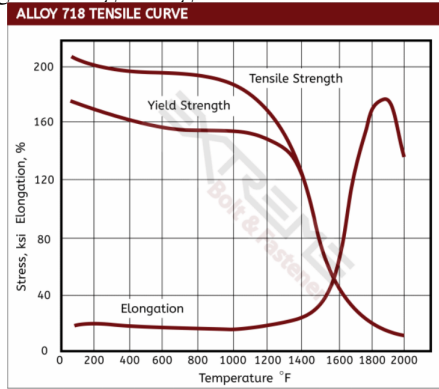


Fig. 14. Inconel 718 strength vs temperature [5]

The maximum coolant temperature of 250F is also well within design specifications as the boiling point of Isopropyl Alcohol at our working pressures is near 400F [6], leaving plenty of margin in terms of the overall heat transferred to the coolant, and good resistance against flow instabilities which onset of bulk flow boiling in the cooling channels could cause. However, subcooled nucleate boiling will still likely occur in the cooling channels as the wall temperature is significantly above the saturation temperature and the engine should be monitored for any instabilities this may cause.

Finally, the predicted pressure drop of 174 psi within the cooling channels is well within the bounds of the pressure budget we can provide using a compressed gas pressurant system.

While this analysis gives confidence in our design, it will not be validated until we can perform physical testing of the prototype. During testing, we will be able to measure the total heat absorbed by the coolant through immersed thermocouples placed just before the inlet to the combustion chamber at the nozzle and in the injector fuel manifold. The difference in temperature observed can then be used in combination with the known coolant specific heat to measure the total heat transfer. Additionally, surface thermocouples on the combustion chamber will give further data to validate and improve our model.

B. Manufacturing

We were extremely impressed with the quality of the part we received, with minimal surface roughness for an additively manufactured part, tight tolerances, and no blocked

orifices or channels. Therefore we determined this part would be acceptable to continue testing with.

C. Cold Flow Testing

Our cold flow testing results were also extremely positive. As we saw no evidence of blocked orifices among the fuel, oxidizer, and combustion chamber manifolds, we are confident that our 3D printed manifold designs were produced as designed. Additionally, good impingement on all the injector elements was seen, again validating the design and manufacturing. Finally, no leaks or crossover between fuel and oxidizer manifolds were observed, giving confidence in the internal structure of the parts.

This confidence in the basic function of all parts will allow these parts to move into the next phase of testing, in which more quantitative data will be gathered such as pressure drops through the fuel and oxidizer sides of the injector, which will give an indication of the exact tolerance to which the injector orifices were printed.

D. Conclusion

We have completed design, manufacturing, and cold flow testing of a unique 3D printed regeneratively cooled nitrous oxide/isopropyl alcohol rocket engine, which when tested will be the first such engine ever fired. The basis for the design was to create a first prototype of an additively manufactured liquid rocket engine that could be used on Columbia Rocketry's entry into the Spaceport America Cup Student Launch Competition. The engine is designed to generate 600 pounds of thrust and can be fired in steady state indefinitely as long as propellants are provided thanks to the implementation of a regeneratively cooled combustion chamber. Our design leverages the novel capabilities afforded by the additive manufacturing process to include numerically optimized cooling channels and flow paths, low mass, and small injector orifices for improved atomization and combustion efficiency.

The injector and combustion chamber were manufactured by 3D Systems using Direct Metal Laser Sintering in Inconel 718, and displayed adequate tolerances and surface finish. Several post-processing steps were also performed to prepare the resulting parts for testing.

Cold flow testing using water was performed on each of the flow pathways, and the resulting flow patterns were analyzed, showing no anomalies and good agreement with the design intent of the assembly.

Moving forward, the engine will be handed off to Columbia Rocketry for continued testing. First, the fuel side fluid systems such as fuel tank, valve, and pressurization system will need to be assembled and tested. Then, further quantitative cold flow testing will need to be performed with propellants to determine working pressure drops. Finally, the engine will need to be integrated with the rocketry teams test stand and tested in hot fire. Additional tests such as static pressurization and leak tests should also be performed before static fire testing. We hope to see wonderful footage of the engine in action during the coming year.

REFERENCES

- [1] M. Watch, "Small Satellite Market Global Forecast 2025," *Marketwatch*, 2019.
- [2] D. Messier, "DLR Developing Reusable Rocket Engine for Small Satellite Launcher," *Parabolic Arc*, 2018.
- [3] B. S. Waxman, B. Cantwell, A. J. Jose, and G. G. Zilliac, *An investigation of injectors for use with high vapor pressure propellants with applications to hybrid rockets*. PhD thesis, 2014.
- [4] D. K. Huzel and D. H. Huang, *Design of Liquid Propellant Rocket Engines Second Edition*. NASA Headquarters Washington, DC: NASA, 1971.
- [5] E. Bolt, "Inconel threaded rods."
- [6] J. S. Parks and B. Barton, "Vapor pressure data for isopropyl alcohol and tertiary butyl alcohol," *Journal of the American Chemical Society*, 1928.